Estimating shortwave radiative forcing and response in climate models

K.E. Taylor,[1*] M. Crucifix,[2]
P. Braconnot,[3] C.D. Hewitt,[2] C. Doutriaux,[1]
A.J. Broccoli,[4] J.F.B. Mitchell[2] and M.J. Webb,[2]

10 October 2006

[1] Program for Climate Model Diagnosis and Intercomparison, L-103, Lawrence Livermore National Laboratory, Livermore, CA 94550, USA.

[2] Hadley Centre for Climate Prediction and Research, U.K. Met. Office, Exeter, UK.

[3] Laboratoire des Sciences du Climat et de l'Environnement, CEA-DSM, Saclay, France.

[4] Rutgers University, New Brunswick, NJ, USA.

[*] To whom correspondence should be addressed. Email: taylor13@llnl.gov (tel: 925 423-3623, fax: 925-422-7675).

Abstract

Feedback analysis in climate models commonly involves decomposing any change in the system's energy balance into radiative forcing terms due to prescribed changes, and response terms due to the radiative effects of changes in model variables such as temperature, water vapor, clouds, sea-ice and snow. The established "partial radiative perturbation" (PRP) method allows an accurate separation of these terms, but requires processing large volumes of model output with an offline version of the model's radiation code. Here, we propose an "approximate PRP" (APRP) method for the shortwave that provides an accurate estimate of the radiative perturbation, but derived from a quite modest amount of monthly mean model output.

The APRP method is based on a simplified shortwave radiative model of the atmosphere, where surface absorption and atmospheric scattering and absorption are represented by means of three parameters that are diagnosed for overcast and clear-sky portions of each model grid-cell. The accuracy of the method is gauged relative to full PRP calculations in two experiments: one in which carbon dioxide concentration is doubled and another in which conditions of the last glacial maximum (LGM) are simulated. The approximate PRP method yields a shortwave cloud feedback accurate in the global mean to within 7%. Forcings and feedbacks due to surface albedo and non-cloud atmospheric constituents are also well approximated with errors of order 5-10 %. Comparison of two different model simulations of the LGM shows that the regional and global differences in their ice

sheet albedo forcing fields are clearly captured by the APRP method. Hence this method is an efficient and satisfactory tool for studying and intercomparing shortwave forcing and feedbacks in climate models.

1. Introduction

When coupled atmosphere-mixed layer ocean models respond to imposed perturbations in atmospheric concentrations of "greenhouse gases" (most commonly CO_2), they predict changes in equilibrium global mean surface temperature that can differ by as much as a factor of two or more (Cubasch et al. 2001). Likewise, models used to simulate the climate of the last glacial maximum produce a range of responses (Masson et al. 2006). The surface temperature changes are, of course, only one facet of the richly complex climatic response, and the interactions among multiple nonlinear processes make it difficult to identify the factors most responsible for the climatic changes simulated by models. Uncovering the reasons for different responses in different models is equally difficult.

In spite of these challenges, we seek to reduce uncertainty in predictions of future climate change, which, at the very least, requires us to identify the processes that most directly lead to the spread of responses. As in the analysis of many complex physical systems, a useful first step is to consider which processes are energetically dominant. It is unlikely, after all, that a process which only weakly affects the energy flow and storage within the system will dominate its response to perturbations. This, then, is the underlying rationale for performing simple "feedback analyses" in which the effects of various aspects of a climate model's response are evaluated in terms of their overall impact on the energy budget of the system. Studies of this kind have led to the recognition that clouds are a major contributor to the uncertainty in future climate projections (Cess et al. 1990, 1996; Senior and Mitchell 1993; Colman 2003; Bony et al. 2006; Webb et al. 2006).

Any imbalance in the global mean fluxes of shortwave and longwave radiation at the top of the atmosphere (TOA) must lead to a change in the energy content of the climate system, which almost inevitably results in a temperature change. The radiative "forcing" of the system is commonly quantified in terms of the immediate impact of any imposed change on the TOA fluxes [1]. An imposed increase in CO_2 concentration, for example, promptly reduces, by a small amount, the longwave radiation emanating to space and is therefore considered a radiative forcing. The radiative imbalance caused by this forcing tends to warm the system, and, in any given model, the global mean temperature response is roughly proportional to the initial radiation imbalance (Hansen et al. 2005). In traditional feedback analyses (Hansen et al. 1984; Schlesinger 1989) the effect of individual aspects of the response (e.g., changes in water vapor, clouds, surface albedo, etc.) on the balance of fluxes of shortwave (SW) and longwave (LW) radiation at the top of the atmosphere are estimated to gauge their relative importance. Some of these effects tend to reinforce the initial TOA perturbation, while others counter it, constituting positive and negative feedbacks, respectively.

One procedure for estimating the feedback strengths was introduced by Wetherald and Manabe (1988) and is now referred to as the "partial radiative perturbation" (PRP) procedure. The PRP method requires multiple calls to a model's radiation code to assess the impact on TOA fluxes of changes in some property of the sys-

[1] Depending on one's perspective, the subsequent analysis can sometimes be simplified if one modifies the definition of feedback to include only those processes governed on time-scales associated with upper ocean response. For example, radiative forcing is often redefined as the flux change at the tropopause after the stratosphere reaches a new radiative equilibrium (under fixed dynamical energy transport), a response that occurs on time-scales much shorter than many other responses. Refinements of this sort can sometimes complicate and confuse the discussion and are avoided here because they do not fundamentally alter the application or evaluation of the feedback methodology described here.

tem, keeping all other properties fixed. The change in an individual property is directly obtained from the two climate states simulated in a climate change experiment. The change in TOA flux, as diagnosed through this procedure, divided by the global mean surface temperature is the usual reported measure of the strength of the radiative feedback associated with the property.

A practical limitation of the PRP method is that it requires storage of high frequency synoptic global fields of surface albedo and profiles of the temperature, water vapor, and cloud and aerosol properties. These fields are typically sampled every 3 hours through a complete annual cycle of both a control and a perturbed simulation. The PRP analysis is then usually performed "offline" (i.e., after completion of the simulations). The model's radiation code is run, first with all properties prescribed consistent with the control simulation, and then, with all but one property taken from the control experiment and the remaining property taken from the perturbed run. The difference in TOA flux between these two calculations yields a measure of the impact of the change in that property on the system's response. The procedure is applied to each time sample, and it must be repeated for each property considered. For N properties, this requires $N+1$ calls to the radiation code for the complete set of spatial and temporal samples. Consequently, considerable computational resources are required, as well as the nontrivial development of computer programs to process the archived fields. Partly for this reason, no one has yet applied a full PRP analysis consistently across models (although Colman (2003) has collected PRP results from many models, derived by various, not completely equivalent means.)

It is primarily because of the practical difficulties in routinely applying the PRP

method that alternative methods of assessing the strength of feedbacks have been sought. Perhaps simplest of these is a method used to assess the importance of cloud responses by considering the change between two climatic states of cloud radiative forcing (CRF), defined as the difference in all-sky and clear-sky fluxes at the TOA (Cess et al. 1990). Zhang et al. (1994), Colman (2003), and Soden et al. (2004) have investigated the differences between the cloud forcing approach and the PRP method, and specifically point out why interpretation of a change in CRF cannot be attributed solely to changes in clouds themselves, but also depends on the "masking" effects of unchanging clouds on the non-cloud feedbacks.

Soden and Held (2005) have used the GFDL model to estimate partial derivatives of the radiative fluxes with respect to temperature, water vapor and surface albedo, and then used these derivatives to approximate the contributions of each variable to radiative response in several other recent coupled model simulations. They thereby obtain estimates of non-cloud feedbacks from these models, while making some allowance for masking effects. The cloud feedbacks are then simply the residual not explained by the non-cloud feedbacks.

Winton (2005) developed several methods for estimating surface albedo feedback based on monthly mean model output. His "four parameter" method was the most accurate but required special zero-albedo surface flux diagnostics not normally available as part of model standard output. Another technique, his "ALL/CLR" method, required only standard diagnostics but was restricted to the surface and did not directly diagnose the impact of surface albedo changes at the top of the atmosphere. Winton (2006) applied the latter method to diagnose the impact of surface albedo changes on the surface shortwave fluxes in recent simulations by

several different models.

Qu and Hall (2006) also developed a technique for estimating surface albedo feedback based on standard model output. The technique was used to assess snow albedo feedback in seventeen climate models.

Of particular relevance to the present study are methods in which model radiative forcings and responses are analysed with simple, single layer radiative transfer models tuned to mimic the more complex original radiation codes (Taylor et al. 2000; Yokohata et al. 2005). Here we elaborate on these methods by providing a theoretical framework that we refer to as approximate PRP (APRP). We will show how APRP may be used to routinely quantify snow, sea-ice and cloud radiative responses, as well as ice sheet albedo forcing imposed in a palaeoclimate experiment. The method is tested and compared with full PRP calculations in two experiments: one in which carbon dioxide concentration is doubled in the atmosphere (2xCO_2) and another in which conditions corresponding to the last glacial maximum (LGM) are prescribed.

In section 2 we formulate the feedback analysis in terms of changes in TOA radiative flux. We then introduce a simple shortwave radiation model that can be used to reproduce some of the radiation fields simulated by the more complex codes found in climate models. This surrogate model allows us to isolate the radiative effects of changes in clouds from changes in surface albedo and other atmospheric constituents. In section 3 we apply and test the ability of this simplified approach to reproduce PRP estimates of surface albedo feedbacks, cloud feedbacks, and feedbacks from changes in other atmospheric properties in a doubled CO_2 experiment. We also use the model to estimate the ice sheet albedo forcing in LGM

experiments, and compare these estimates with more exact calculations. Our conclusions and further discussion appear in section 4.

2. Method

2a. *Definition of radiative response*

The net radiative flux across the top of the atmosphere (TOA), along with horizontal transports, determines the rate of change of vertically integrated energy in the climate system:

$$\frac{\partial E}{\partial t} + \nabla \cdot \vec{v}E = R \equiv Q + F. \tag{1}$$

The left hand side of (1) accounts for changes in energy storage (E) and also horizontal energy transport ($\vec{v}E$) in a column extending from the top of the atmosphere to below the Earth's surface. Q is the net downward shortwave flux at the TOA, F is the negatively signed outgoing longwave radiation, and R is their sum.

Any perturbation to the net TOA flux, represented by the right hand side of (1), forces changes in the storage and transport terms. A perturbation in TOA flux that has been essentially imposed is labeled a "radiative forcing," as discussed earlier. Some aspects of the subsequent responses of climate may also affect the fluxes, and individually they may either enhance or reduce the initial TOA radiative flux perturbation. We refer to those aspects of the system's response that directly affect the TOA balance as "radiative response". Thus,

$$\Delta R = \Delta R_{\mathrm{f}} + \Delta R_{\mathrm{r}} \tag{2}$$

where the TOA perturbations due to forcing, radiative response, and their sum are represented by ΔR_{f}, ΔR_{r}, and ΔR, respectively. In PRP studies the radiative response is often normalized by the global mean surface temperature change (i.e., $\Delta R_{\mathrm{r}}/\Delta T$), which is called the radiative feedback parameter.

According to (2), not all aspects of climate response are considered radiative responses – only those that impact the TOA fluxes directly. A change in surface evaporation, for example, does not directly affect TOA radiation, yet may be considered an important part of the climate response. It can directly affect water vapor concentration, which, of course, does have an impact on the TOA fluxes. Only the water vapor feedback itself, however, can be quantified through radiative feedback analysis, not the changes in sources, sinks, and atmospheric transport that led to the changes in water vapor.

Although a radiative feedback analysis of this sort is not meant to penetrate the full complexity of the climate's response, it can be used to identify those aspects of the response that have the most important direct impact on the planet's energy balance. Once the most important radiative responses are identified by this initial step, more incisive diagnostics must be applied to understand the processes that determine that response (Stephens 2005). In short, the value of radiative feedback analysis is the guidance it provides in prioritizing which processes might be most fruitfully analyzed in further detail.

In summary, changes in TOA radiative fluxes can result both from internal re-

sponses and from imposed changes in conditions that result in radiative forcing. In the next two subsections these two elements affecting the TOA fluxes will be treated without distinction, but in later subsections they will again be considered separately.

2b. *Treatment of partially overcast regions.*

In model simulations, the net TOA flux of radiation (and also the individual SW and LW components) simulated by a model can be resolved into two terms:

$$R = (1-c)R_{\mathrm{clr}} + cR_{\mathrm{oc}} \tag{3}$$

where c is the fraction of the region occupied by clouds, R_{clr} the spatially averaged flux resulting from clearing all clouds from the region and repeating the radiative transfer calculation, and R_{oc} the flux averaged over only the overcast portion of the region.

The change in R (i.e., ΔR) between two states, s_1 and s_2 (representing, for example, two different times or two different mean climates), can, without approximation, be written:

$$\begin{aligned} \Delta R \equiv R_2 - R_1 &= (1-c)\Delta R_{\mathrm{clr}} + c\Delta R_{\mathrm{oc}} + \Delta c(R_{\mathrm{oc}} - R_{\mathrm{clr}}) \\ &= \Delta R_{\mathrm{clr}} + \Delta c(R_{\mathrm{oc}} - R_{\mathrm{clr}}) + c(\Delta R_{\mathrm{oc}} - \Delta R_{\mathrm{clr}}) \end{aligned} \tag{4}$$

where in the absence of the "Δ" symbol and in the absence of an integer subscript,

the value is taken to represent the mean of the two states (e.g., $c = (c_1 + c_2)/2$)). If the region is cloud free for s_1 but not s_2, then $R_{1\mathrm{oc}}$ is undefined and we shall set $R_{1\mathrm{oc}} = R_{2\mathrm{oc}}$ (and similarly for the converse case). If the region is cloud free in both states, then $\Delta R = \Delta R_{\mathrm{clr}}$.

It should be noted that (4) is perfectly general in the sense that the two states it assumes need not be equilibrium states. The last three terms in (4) represent, respectively, the flux change not considering the effects of clouds, a contribution from changing cloud fraction (but with all other properties affecting radiation held fixed), and the differential change due to the presence of clouds (but with total cloud fraction held fixed). The sum of the last two terms superficially appears to represent the effects of changing clouds (after all in the absence of clouds each would be zero). It is equivalent to the change in "cloud forcing" (see, .e.g., Cess et al. (1990)). As discussed by Soden et al. (2004), however, it is not correct to consider this change in cloud forcing to be an accurate measure of "cloud feedback". In fact, the last term will not vanish, even if clouds themselves are unchanged, provided that clear-sky conditions (represented by ΔR_{clr}) change. Also, ΔR may in general include a contribution from an imposed radiative forcing (e.g., increased CO_2 concentration), which may also differ between clear and overcast portions of a grid-cell.

2c. *An approximate PRP method for shortwave analysis.*

The APRP method involves evaluation of various contributions to changes in the TOA net shortwave radiation, so the first step is to express the net flux in terms of

the insolation, S, and the planetary albedo, A:

$$Q = S(1 - A). \tag{5}$$

This and other formulas in this subsection apply not only to the total ("all-sky") flux, but also to its clear-sky and overcast components. A change in the shortwave flux can also be resolved into two components, one representing the contribution from changes in insolation, the other, changes in planetary albedo:

$$\Delta Q = \Delta S(1 - A) - S\Delta A, \tag{6}$$

where the notation is the same as in (4).

The first term on the right hand side vanishes in most cases, but it could be an important contributor to forcing, if, for example, one were to consider solar cycle variations or changes in the Earth's orbital characteristics.

The last term in (6) represents all the forcings and responses that can affect planetary albedo, including surface albedo and absorption and scattering by the atmosphere.[2] In PRP analyses the importance of each component of the response is determined with offline calculations performed by the climate model's radiation code. Here, following an approach first introduced in Taylor et al. (2000), which was inspired by earlier work by Foley et al. (1991), Covey et al. (1991)

[2]Note that planetary albedo cannot be determined when the insolation is 0, but we proceed similarly to our treatment of undefined overcast fluxes in (4): if $S_1 = 0$, but $S_2 \neq 0$, then set $A_1 = A_2$ (and similarly for the converse case); also, if $S_1 = S_2 = 0$, then $\Delta Q = 0$, as are the terms comprising it.

and Murphy (1995), we decompose forcings and responses relying on a simple radiative transfer model that can be tuned to mimic in some respects the behavior of a climate model's full radiative transfer code. Once this is done, the parameters in the simple model are perturbed individually by the amount that they change in the climate response, and the APRP result is obtained with the simple radiative transfer model in a manner completely analagous to calculating a PRP result in a more complex climate model.

The properties that determine changes in planetary albedo can be simply represented, at least conceptually, in a single layer model of the atmospheric column shown in Figure 1. The single atmospheric layer scatters radiation passing downward or upward through it, but absorbs radiation only on the incident radiation's first transit (after which the energy in the spectral bands where significant absorption occurs is assumed to be substantially depleted). Note that ozone absorption is well approximated by this model because nearly all the radiation in its absorption bands is removed before reaching the troposphere. For a strongly absorbing tropospheric aerosol, on the other hand, this simplified model would likely be less accurate. The neglect of atmospheric absorption of SW radiation reflected by the surface is supported by Figure 3 in Winton (2006), which shows that the upward beam absorptivity is several times smaller than the downward beam absorptivity.

[Figure 1 about here.]

According to this simplified shortwave model, the planetary albedo (A) and the ratio ($\hat{Q}_s^{\downarrow}$) of incident surface flux to the insolation, are given by the following

formulas:

$$
\begin{aligned}
A &= \mu\gamma + \mu(1-\gamma)^2\alpha(1+\alpha\gamma+\alpha^2\gamma^2+\cdots) \\
&= \mu\gamma + \frac{\mu\alpha(1-\gamma)^2}{1-\alpha\gamma} \qquad (7) \\
\hat{Q}_s^{\downarrow} &= \mu(1-\gamma)(1+\alpha\gamma+\alpha^2\gamma^2+\cdots) \\
&= \frac{\mu(1-\gamma)}{1-\alpha\gamma} \qquad (8)
\end{aligned}
$$

The values of α, γ and μ, which in general vary spatially and with time, can be chosen to yield surface and TOA fluxes that match those simulated by more realistic radiation codes found in contemporary climate models. The upwelling and downwelling streams of radiation simulated by those models yield three independent flux ratios that determine α , γ and μ. These flux ratios are the planetary albedo ($A = 1 - Q/S$), the surface albedo ($\alpha = Q_s^{\uparrow}/Q_s^{\downarrow}$), and the ratio of incident surface flux to the insolation ($\hat{Q}_s^{\downarrow}$). The fraction of incident radiation absorbed by the atmosphere ($1-\mu$) is, by definition, the difference between the shortwave radiation absorbed by the combined atmosphere and surface system and the net flux absorbed at the surface alone. Thus,

$$1-\mu = 1 - A - \hat{Q}_s^{\downarrow}(1-\alpha),$$

which yields:

$$\mu = A + \hat{Q}_s^{\downarrow}(1-\alpha). \qquad (9)$$

Finally, the scattering coefficient, γ, can be calculated from μ, α and $\hat{Q}_s^{\downarrow}$, using

(8):

$$\gamma = \frac{\mu - \hat{Q}_s^{\downarrow}}{\mu - \alpha \hat{Q}_s^{\downarrow}}. \tag{10}$$

If the incident and reflected shortwave radiation at the surface and the top of the atmosphere are saved as output from a climate model, we can use the definition of surface albedo along with (9) and (10) to calculate the values of α, μ and γ that ensure the fluxes simulated by our simplified model match those of the more sophisticated model.

Having developed a simplified representation of the climate model's actual treatment of radiation, we can perform a PRP analysis of the surrogate. The dependence of the last term in (6), $S\Delta A$ may be estimated by decomposing (7) in the following form :

$$\Delta A = \frac{\partial A}{\partial \alpha}\Delta\alpha + \frac{\partial A}{\partial \mu}\Delta\mu + \frac{\partial A}{\partial \gamma}\Delta\gamma + \Delta A_{\mathrm{NL}}, \tag{11}$$

where the last term accounts for nonlinear, higher order effects. Each of the terms in (11) can be estimated from output of control and perturbed climate model simulations (or, when analyzing the climatological annual variation of feedbacks, from the output of a single simulation). The first term on the right hand side can be computed, for example, as follows:

$$\frac{\partial A}{\partial \alpha}\Delta\alpha \approx \frac{\Delta A_\alpha}{\Delta\alpha}\Delta\alpha = \Delta A_\alpha \equiv A(\mu,\gamma,\alpha_2) - A(\mu,\gamma,\alpha_1) \tag{12a}$$

where the subscripts "1" and "2" refer to the control and perturbation simulations, respectively, and in the absence of a subscript, the parameters are assigned the mean of the control and perturbed values [3]. Similar formulas apply to the other linear terms in (11), and the last term can be computed as a residual by subtracting the three linear terms from the total change in planetary albedo given by $\Delta A = A(\mu_2, \gamma_2, \alpha_2) - A(\mu_1, \gamma_1, \alpha_1)$. When using (12a), (12b), and (12d), ΔA_{NL} is a third order term in the perturbation quantities, whereas in the case of (12c), it is a second order term.

To isolate the effects associated with clouds from those of the other atmospheric constituents, we can resolve the radiative fluxes into their clear-sky and overcast components as in (3). We then separately calculate the clear-sky and overcast values of the three parameters, α, γ, and μ, based on the radiative fluxes in clear-sky and overcast regions, respectively. Note that the overcast flux is inferred, using (3), from the total and clear-sky fluxes, which are commonly saved as part of the standard output of model simulations.

Next we make the assumption that in overcast regions, the non-cloud atmospheric constituents absorb and scatter the same proportion of the radiation stream as they would if clouds were abruptly cleared from the region. This approximation will be

[3] Alternatively, ΔA_α can be estimated in any one of the following ways:

$$\Delta A_\alpha = \frac{1}{2}\left(A\left(\mu_1, \gamma_1, \alpha_2\right) - A\left(\mu_1, \gamma_1, \alpha_1\right)\right) + \frac{1}{2}\left(A\left(\mu_2, \gamma_2, \alpha_2\right) - A\left(\mu_2, \gamma_2, \alpha_1\right)\right) \tag{12b}$$

$$\Delta A_\alpha = \left(A\left(\mu_i, \gamma_i, \alpha_2\right) - A\left(\mu_i, \gamma_i, \alpha_1\right)\right), \quad \text{where } i = 1 \text{ or } i = 2 \tag{12c}$$

$$\Delta A_\alpha = \left(\alpha_2 - \alpha_1\right) \left.\frac{\partial A}{\partial \alpha}\right|_{\mu=\frac{1}{2}(\mu_1+\mu_2);\gamma=\frac{1}{2}(\gamma_1+\gamma_2);\alpha=\frac{1}{2}(\alpha_1+\alpha_2)} \tag{12d}$$

where, in (12d), the derivative is calculated analytically using (7). Equation 12b represents the estimate obtained by doing both a *forward* and *backward* substitution, as decribed by Colman (2003).

most accurate when atmospheric absorption and scattering is weak (thin optical depth) or if the cloud and non-cloud constituents affect different wavelengths. Limitations of this approximation will be reflected in errors in the APRP method (see section 3).

Under the approximation just discussed, the scattering coefficient in the overcast portion of the grid-cells (γ_{oc}) can be expressed as a combination of a clear-sky coefficient and a scattering coefficient due to the cloud itself:

$$(1-\gamma_{oc}) = (1-\gamma_{clr})(1-\gamma_{cld}). \tag{13}$$

As γ_{oc} and γ_{clr} can be calculated from (10), based on the appropriate overcast and clear-sky fluxes, γ_{cld} is simply diagnosed using (13). Similarly, the coefficients for the absorption by non-cloud atmospheric constituents is assumed to be unaffected by the presence or absence of a cloud, so

$$\mu_{oc} = \mu_{clr}\mu_{cld}, \tag{14}$$

and surface albedo may differ between clear-sky and overcast conditions (designated, α_{clr} and α_{oc}) due to differing contributions of direct beam and diffuse incident radiation.

Once the optical properties have been determined, the planetary albedo,

$$A = (1-c)A_{clr} + cA_{oc} \tag{15}$$

can be expressed as a function of seven parameters:

$$A = A(c, \alpha_{\mathrm{clr}}, \alpha_{\mathrm{oc}}, \mu_{\mathrm{clr}}, \mu_{\mathrm{cld}}, \gamma_{\mathrm{clr}}, \gamma_{\mathrm{cld}}).$$

The radiative responses associated with changes in surface albedo and changes in the cloud and non-cloud constituents of the atmosphere can then be estimated (following the notation of (12a-d)):

$$\Delta A_{\alpha} = \Delta A_{\alpha_{\mathrm{clr}}} + \Delta A_{\alpha_{\mathrm{oc}}} \tag{16a}$$

$$\Delta A_{\mathrm{cld}} = \left(\Delta A_{\mu_{\mathrm{cld}}} + \Delta A_{\gamma_{\mathrm{cld}}}\right) + \Delta A_{c} \tag{16b}$$

$$\Delta A_{\mathrm{clr}} = \left(\Delta A_{\mu_{\mathrm{clr}}} + \Delta A_{\gamma_{\mathrm{clr}}}\right) \tag{16c}$$

These equations, which quantify the surface albedo, cloud, and non-cloud atmospheric radiative responses, constitute the shortwave APRP method. The terms on the right hand side of (16b) can be individually evaluated to determine the relative importance to radiative response of changes in scattering, absorption, and total cloud fraction. Likewise, the masking effects of clouds on surface albedo changes can be inferred, with the help of (15), from the two terms in (16a).

The method is largely as described in Taylor et al. (2000), but with an improved separation of cloud and non-cloud effects in the overcast portions of grid cells using equations (13) and (14). These relationships are similar to those proposed by Yokohata et al. (2005), but ours apply only to the portion of the grid cell that is overcast, whereas in their approach the overcast and clear-sky portions of grid-cells are not treated separately. Variations in their cloud scattering and absorption

properties must therefore reflect the combined effect of variations in the extent of the clouds (i.e., cloud fraction) and variations in cloud optical properties. In contrast, the decomposition expressed in (16b), explicitly isolates the effect of changes in cloud extent, so that in our case $\gamma_{\rm cld}$ and $\mu_{\rm cld}$ are determined solely by the cloud optical properties.

3. Verification of the approximate PRP method.

Here we assess the accuracy of the shortwave APRP method. Two tests are performed. First, for a single model we analyze the surface albedo and shortwave cloud radiative responses in doubled CO_2 experiments. Then, for two different model simulations of last glacial maximum conditions, we test how accurately shortwave APRP can estimate radiative forcing due to the surface albedo changes implied by the prescription of continental-scale ice-sheets. In each case, to gauge the accuracy of the shortwave APRP estimate, we compare it with more exact PRP calculations. The PRP estimates are based on the "two-sided" analysis introduced by Colman and McAvaney (1997) to reduce the influence of the so-called "decorrelation perturbation."

3a. *Shortwave feedbacks in doubled CO_2 experiments.*

We use model output fields from a "slab-ocean" experiment carried out with the GFDL AM2 climate model (The GFDL Global Atmospheric Model Development Team (2004)). In this experiment the CO_2 concentration is doubled with respect

to a control (pre-industrial climate) state. The model is integrated until an equilibrium is reached (i.e., until the net TOA radiation balance is restored), so that in (2), $\Delta R = 0$. Therefore, the longwave and shortwave forcings induced by the CO_2 doubling causes a radiative response that exactly compensates for the forcing. For this model, the balance is achieved once the globally averaged, annual mean temperature increases by 2.7 K. In this section, the shortwave component of the radiative response is decomposed using the APRP method presented in section 2 (using monthly mean outputs), and the results are then compared to PRP calculations provided by Brian Soden (personal communication). Table 1 provides a summary of the comparison between APRP and PRP estimates of the global mean radiative responses. Note that the "non-cloud" terms actually include the CO_2 shortwave forcing of 0.29 Wm^{-2}.

[Table 1 about here.]

Figure 2a shows the APRP estimate of the radiative response due to changes in surface albedo, calculated using (16a) and based on the monthly mean climatology of the simulations. The globally averaged, annual mean response is 0.72 Wm^{-2}. In comparison, the proper PRP estimate of the albedo radiative response is 0.79 Wm^{-2}, so the APRP error is about 10%. Figure 2b shows that the local errors are mostly less than 1 Wm^{-2} in magnitude and that these are mostly in locations where the actual response is between 2 and 8 Wm^{-2}. The correlation between the APRP and the PRP spatial patterns of the surface albedo feedback is 0.997.

[Figure 2 about here.]

The comparison between APRP estimates can also be made with somewhat less accuracy using an annual mean climatology, rather than the monthly mean climatolgy. If this is done in the case of the surface albedo feedback, the global mean is estimated to be 0.69, which is within about 13% of the PRP value. The RMS error in the spatial distribution of the feedback based on annual mean climatology is, however, about 70% larger than that based on the monthly mean climatology. Thus, at the regional scale the monthly mean climatology provides a much better estimate of the radiative response to surface albedo changes.

Considering next the APRP shortwave cloud feedback (Figure 3a), we find an annual mean, global mean value of -0.67 Wm^{-2}. When gauged against PRP, the approximate PRP performs well (Figure 3b), with an error in the mean of -0.04 Wm^{-2}, a root-mean-square (RMS) error of 0.39 Wm^{-2}, and a correlation of 0.997. Notably, the cloud feedback over sea-ice is captured quite accurately.

[Figure 3 about here.]

The PRP estimate can also be compared to the change in cloud forcing, as given by the sum of the last two terms of (4). The difference between the cloud forcing change and the PRP cloud feedback response is shown in Figure 3c. The global mean difference is of the same order of magnitude (-0.25 Wm^{-2}) as the cloud feedback response itself. The RMS error (taking the PRP estimate as truth) is 2.0 Wm^{-2}, more than five times the APRP error. In 3c, the largest differences are found over sea-ice and northern high-latitudes, which is expected because these are the regions where the surface albedo changes are particularly large. Even where surface albedo is essentially unchanged, however, there are differ-

ences. Relative to the cloud forcing change, the APRP method results in generally smaller errors over snow-free and ice-free regions. One plausible explanation for this is that the SW cloud forcing will change as the climate warms, even if the clouds themselves are unchanged. Increases in water vapor in a warmer climate will enhance clear-sky absorption of water vapor, but this enhancement will be weaker when clouds are present because the incident SW below the cloud will be reduced by cloud reflection. This effect may be responsible for the systematic over-estimate of SW cloud radiative response throughout the low latitudes seen in Figure 3c. To determine the validity of this hypothesis, a PRP calculation could be done in which only the water vapor is increased (by the amount seen in the doubled CO_2 simulation) and the effect on TOA fluxes is assessed in both clear-sky and overcast regions. Regardless of the reasons for the discrepancies between the cloud forcing change and the PRP diagnosis, these results reinforce the view that changes in cloud forcing cannot be relied upon to accurately quantify the cloud feedback. In contrast, the APRP method is much more accurate.

Finally, we note that the APRP estimate of the response due to atmospheric constituents other than clouds (e.g. water vapor, aerosols, etc.) is about 10% higher than the PRP value (1.24 Wm^{-2} rather than 1.15 Wm^{-2})

It is further instructive to compare the performance of our APRP method with an alternative used in Yokohata et al. (2005). In the experiment analyzed here, the Yokohata et al. (2005) approach yields a globally averaged error in estimating cloud feedback of 0.80 Wm^{-2} (compared with the APRP error of about -0.04 Wm^{-2}). The RMS error (0.91 Wm^{-2}) is also more than twice as large as the error resulting from our APRP method. The differences between our shortwave APRP

method and that of Yokohata et al. (2005) are: (i) our radiative model considers scattering on multiple upward and downward paths, (ii) absorption occurs only on the first incoming radiation path, and (iii) overcast and clear-sky portions of the grid-cell are treated separately.

3b. *PMIP last glacial maximum forcing results.*

During the LGM (ca. 21,000 years ago), temperatures were lower than at present because concentrations of main greenhouse gases were lower and because the surface albedo was higher due to the extensive ice sheets covering regions of North America and Scandinavia. The LGM has therefore long been chosen as a reference period to study large scale climate feedbacks (Hansen et al. 1984; Hewitt and Mitchell 1997). The Palaeoclimate Modelling Intercomparison Project (PMIP, Joussaume and Taylor (2000); `http://www-lsce.cea.fr/pmip`) has archived model output from a series of standardized experiments performed with seventeen different climate models. For our purposes, however, special PRP calculations are required, which are available from only two of those models, identified here as the "GFDL" (Broccoli 2000) and "UKMO" (Johns et al. 1997) models. Among the PMIP experiments are a present-day control ("0cal") and an LGM simulation ("21cal"), both performed with the "slab-ocean" versions of the climate models. The "21cal" experiments differ from "0cal" in three important ways: (i) the land-sea mask, land-ice mask, and orography were altered, consistent with the Peltier (1994) reconstruction, (ii) certain greenhouse gas concentrations were reduced, consistent with LGM conditions, and (iii) earth orbital parameters were adjusted according to (Berger 1978). Further details of the experimental setup and results

of the project are available at the website referenced above.

The shortwave forcing is defined as the change in the net downward shortwave flux at the top of the atmosphere resulting from changes in insolation plus changes in surface albedo resulting from changes in the land-sea and land-ice masks. The ice sheet forcing is the contribution to the shortwave forcing of a change in land-ice mask.

[Figure 4 about here.]

The spatial distribution of the PRP diagnosis of ice sheet shortwave forcing for the GFDL and UKMO models is displayed in Figure 4 (panels a and c). Two major features, which are common to the two models, are evident: (i) the forcing is negative where ice has replaced bare or vegetated soil, and (ii) the forcing amplitude is larger on the southern edge of the ice sheets both because annual mean insolation is larger there than at higher latitudes and because the surface albedo change resulting from the LGM ice sheet is larger where there is less snow in the control simulation (0cal). There is, however, a difference in the global mean ice sheet forcing: -2.4 W/m^2 in the GFDL model compared with -2.9 W/m^2 in the UKMO model. The model differences are primarily due to differences in surface albedo formulation and cloud masking effects. Note that the forcing is approximately zero over much of Greenland because the ice sheet still exists there today.

The APRP method, calculated using (16a), again provides a satisfactory approximation to the PRP diagnosed forcing; the APRP estimates of global mean ice sheet forcing in the GFDL and UKMO models are -2.55 W/m^2 and -3.05 W/m^2, re-

specively. Thus, the PRP diagnosed difference of 0.5 W/m^2 is reproduced by the APRP estimate, although this is partly due to a cancelation of slight overestimates of the forcing in both models.

Figure 4 shows that the spatial distribution of the forcing is also accurately estimated by APRP in each model, and, more importantly, the PRP diagnosed differences between the two models is replicated well by the APRP estimate (compare figures 4e and 4f). Confining our attention to the areas covered with glacial ice in one or both of the models, the correlation between the forcing fields shown in figures 4e and 4f is 0.95. Thus, APRP enables us to accurately quantify differences in the patterns of forcing in the two models.

Alhough PRP calculations of ice sheet forcing are not available from the other PMIP models, for several of the models the full set of output needed for an APRP estimate has been archived. For these models, the spread in ice sheet forcing, estimated with APRP, is considerable, ranging from -3.3 W/m^2 at one extreme to -2.0 W/m^2 at the other.

The shortwave APRP method may be used to isolate the contributions of some of the other shortwave forcing components in the LGM experiments. It is found, for example, that differences in sea level lead to a change in the relative areas of land and sea, affecting surface albedo and contributing 10-20 % to the total shortwave forcing. Insolation changes, on the other hand, have much less impact, contributing less than 2%. As in the 2xCO_2 experiments, the shortwave APRP can also provide an estimate of the individual components of radiative response, including snow, sea ice and cloud changes.

With our APRP method, shortwave forcing and feedback terms, based on monthly mean standard model output, can be accurately estimated. Thus, in experiments involving prescribed changes in ice sheets, it is now possible to estimate both shortwave forcing and various shortwave feedbacks. An analysis of this kind appears, for example, in Crucifix (2006).

4. Conclusions

The approximate partial radiative perturbation (APRP) method presented here allows shortwave forcing and feedback terms in climate models to be separated into various components in a manner conceptually equivalent to that of the full PRP method. For many purposes APRP's advantages over the PRP method should more than offset its approximate nature; the differences between global mean APRP estimates and a full PRP diagnosis are typically only a few percent and an order of magnitude smaller than the difference observed between different models.

The major advantage of APRP over full PRP is that it requires only a modest amount of data; the required monthly mean clear-sky and full-sky radiative flux field at the surface and top of the atmosphere are all available as standard diagnostics in model intercomparison databases. Also, unlike the PRP calculation, the computational burden of the APRP calculation is negligible.

The shortwave APRP method combines the simplicity of the cloud forcing method of Cess et al. (1990) with the accuracy of the PRP method, the latter being more suitable for quantifying the individual effects of various forcing and feedback

components in climate change experiments. It is still the case, however, that for comparisons of model simulations with satellite observations, the cloud radiative forcing concept remains useful.

In contrast to the shortwave analysis, accurate separation of longwave forcings and feedbacks using an APRP approach remains challenging. One reason for this is that the TOA fluxes of LW radiation are sensitive to the vertical profiles of clouds, water vapor, and temperature. While Yokohata et al. (2005) proposed a longwave APRP method, they concluded that the difference between their method and the longwave cloud forcing method was small. Given that longwave APRP methods do not at present show a distinct advantage over the longwave cloud forcing method, we recommend the continued use of the cloud forcing method (keeping in mind its limitations) in cases where full PRP calculations (or those based on the method of Soden and Held (2005)) are impractical.

We also hope that the accuracy of the shortwave APRP method demonstrated here will spur its routine use in the analysis of climate change simulations. One difficulty for its general use is that shortwave forcing unrelated to surface albedo changes must be calculated. In the case of carbon dioxide changes, this forcing is relatively small, but not entirely negligible. In experiments involving substantial forcing by aerosols, calculation of the aerosol forcing would be essential, but this is not usually done. Since radiative forcing is not typically calculated, it can be argued that modeling groups should continue to perform idealized standard experiments (in which, for example CO_2 concentration is doubled or increased by 1%/yr), which will allow the relative strengths of the shortwave feedbacks to be determined without estimating the forcing of a complex suite of forcing agents.

Standard experiments of this kind can then be used to help uncover the reasons for the differences in model responses to more realistic forcing scenarios.

There are two further points that deserve mention. First, even though our examples here have both involved equilibrium climate change experiments, the APRP approach is perfectly well suited for the analysis of transient experiments. Thus, the possibly changing strength of different feedbacks can be monitored as the climate evolves. Second, regional APRP estimates are only slightly less accurate than global mean estimates. Consequently, it should now be possible to enhance the approach of Boer and Yu (2003) so that the regional impact of cloud, surface alebedo and non-cloud shortwave feedbacks are more accurately characterized.

Acknowledgements

We are grateful to Brian Soden, who kindly provided us with PRP results from the GFDL model. Work at the University of California, Lawrence Livermore National Laboratory was supported under the auspices of the U.S. Department of Energy Office of Science, Climate Change Prediction Program, under contract No. W-7405-ENG-48.

References

Berger, A. L., 1978: Long-term variations of daily insolation and quaternary climatic. *J. Atmos. Sci.*, **35**.

Boer, G. J. and B. Yu, 2003: Climate sensitivity and climate state. *Clim. Dyn.*, **21**, 167–176.

Bony, S., R. Colman, V. M. Kattsov, R. P. Allan, C. S. Bretherton, J.-L. Dufresne, A. Hall, S. Hallegatte, M. M. Holland, W. J. Ingram, D. A. Randall, B. J. Soden, G. Tselioudis, and M. J. Webb, 2006: How well do we understand and evaluate climate change feedback processes? *J. Climate*, **19**, 3445–3482.

Broccoli, A. J., 2000: Tropical cooling at the Last Glacial Maximum: an atmosphere-mixed layer ocean model simulation. *J. Climate*, **13**, 951–976.

Cess, R. D., G. L. Potter, J. P. Blanchet, G. J. Boer, A. D. Delgenio, M. Dequé, V. Dymnikov, V. Galin, W. L. Gates, S. J. Ghan, J. T. Kiehl, A. A. Lacis, H. Le Treut, Z. X. Li, X. Z. Liang, B. J. McAveney, V. P. Meleshko, J. F. B. Mitchell, J. J. Morcrette, D. A. Randall, L. Rikus, E. Roeckner, J. F. Royer, U. Shlese, D. A. Sheinin, A. Slingo, A. P. Sokolov, K. E. Taylor, W. M. Washington, R. T. Wetherald, I. Yagai, and M. H. Zhang, 1990: Intercomparison and interpretation of climate feedback processes in 19 atmospheric general circulation models. *J. Geophys. Res.*, **95**, 16601–16615.

Cess, R. D., M.-H. Zhang, W. J. Ingram, G. L. Potter, V. Alekseev, H. W. Barker, E. Cohen-Solal, R. A. Colman, D. A. Dazlich, A. D. Del Genio, M. R. Dix, V. Dymnikov, M. Esch, L. D. Fowler, J. R. Fraser, V. Galin, W. L. Gates, J. J. Hack, J. T. Kiehl, H. L. Treut, K. K.-W. Lo, B. J. McAvaney, V. P. Meleshko,

J.-J. Morcrette, D. A. Randall, E. Roeckner, J.-F. Royer, M. E. Schlesinger, P. V. Sporyshev, B. Timbal, E. M. Volodin, K. E. Taylor, W. Wang, and R. T. Wetherald, 1996: Cloud feedback in atmospheric general circulation models: An update. *J. Geophys. Res.*, **101**, 12791–12794.

Colman, R., 2003: A comparison of climate feedbacks in general circulation models. *Clim. Dyn.*, **20**, 865–873.

Colman, R. A., and B. J. McAvaney, 1997: A study of general circulation model climate feedbacks determined from perturbed sea surface temperature experiments. *J. Geophys. Res*, **102**, 19383-19402.

Covey, C., K. E. Taylor, and R. E. Dickinson, 1991: Upper limit for sea ice albedo feedback contribution to global warming. *J. Geophys. Res.*, **96**, 9169–9174.

Crucifix, M., 2006: Does the Last Glacial Maximum constrain climate sensitivity? *Geophys. Res. Lett.*, **33**, L18701, doi:10.1029/2006GL027137.

Cubasch, U., G. A. Meehl, G. J. Boer, R. J. Stouffer, M. Dix, A. Noda, C. A. Senior, S. C. B. Raper, and K. S. Yap, 2001: Projections of future climate change. *Climate change 2001: The scientific basis. Contribution of Working Group I to the Third Assessment Report of the Intergovernmental Panel on Climate Change*, J. T. Houghton, Y. Ding, D. J. Griggs, M. Noguer, P. van der Linden, X. Dai, K. Maskell, and C. I. Johnson, eds., Cambridge University Press, 525–582.

Foley, J. A., K. E. Taylor, and S. J. Ghan, 1991: Planktonic dimethylsulfide and cloud albedo - an estimate of the feedback response. *Clim. Change*,**18**, 1–15.

Hansen, J., M. Sato, R. Rudy, L. Nazarenko, A. Lacis, G. A. Schmidt, G. Russel, I. Aleinov, M. Bauer, S. Bauer, N. Bell, B. Cairns, V. Canuto, M. Chandler, Y. Cheng, A. Del Genio, G. Faluvegi, E. Fleming, A. Friend, T. Hall, C. Jackman, M. Kelley, N. Kiang, D. Koch, J. Lean, J. Lerner, K. Lo, S. Menon, R. Miller, A. Romanou, D. Shindell, P. Stone, S. Sun, N. Tausnev, D. Thresher, B. Wielicki, T. Wong, M. Yao, and S. Zhang, 2005: Efficacy of climate forcings. *J. Geophys. Res.*, **110**, D18104, doi:10.1029/2005JD005776.

Hansen, J. E., A. Lacis, D. Rind, L. Russell, and others, 1984: Climate sensitivity: analysis of feedback mechanisms. *Climate Processes and Climate Sensitivity*, J. E. Hansen and T. Takahashi, eds., American Geophysical Union, 130–163.

Hewitt, C. D. and J. F. B. Mitchell, 1997: Radiative forcing and response of a GCM to ice age boundary conditions: Cloud feedback and climate sensitivity. *Clim. Dyn.*, **13**, 821–834.

Johns, T. C., R. E. Carnell, J. F. Crossley, J. M. Gregory, J. F. B. Mitchell, C. A. Senior, S. F. B. Tett, and R. A. Wood, 1997: The second Hadley Centre coupled ocean-atmosphere GCM: Model description, spinup and validation. *Clim. Dyn.*, **13**, 103–134.

Joussaume, S. and K. E. Taylor, 2000: The paleoclimate modelling intercomparison project. *Paleoclimate Modelling Intercomparison Project(PMIP): Proceedings of the Third PMIP Workshop*, P. Braconnot, ed., *WCRP Report WCRP-111*, WMO/TD No. 1007, 9–24.

Masson, V., M. Kageyama, P. Braconnot, S. Charbit, G. Krinner, C. Ritz, E. Guilyardi, G. Hoffman, J. Jouzel, A. Abe-Ouchi, M. Crucifix, R. Gladstone, C. D. Hewitt, A. Kitoh, A. Legrande, O. Marti, U. Merkel, T. Moto, R. Ohgaito,

B. Otto-Bliesner, W. R. Peltier, I. Ross, P. J. Valdes, G. Vettoretti, S. L. Weber, and F. Wolk, 2006: Past and future polar amplification of climate change: climate mode intercomparison and ice-core constraints. *Clim. Dyn.*, **26**, 513–529.

Murphy, J. M., 1995: Transient response of the Hadley Centre coupled ocean-atmosphere model to increasing carbon dioxide: Part III. Analysis of global-mean response using simple models. *J. Climate*, **8**, 496–514.

Peltier, W. R., 1994: Ice age palaeotopography. *Science*, **265**, 195–201.

Qu, X. and A. Hall, 2006: Assessing snow albedo feedback in simulated climate change. *J. Climate*, **19**, 2617–2630.

Schlesinger, M. E., 1989: *Quantitative analysis of feedbacks in climate model simulations*, American Geophysical Union, Washington D. C., volume 52 of *Geophysical monograph*. 177–187.

Senior, C. A. and J. F. B. Mitchell, 1993: Carbon dioxide and climate: The impact of cloud parameterization. *J. Climate*, **6**, 393–418.

Soden, B. J., A. J. Broccoli, and R. S. Hemler, 2004: On the use of cloud forcing to estimate cloud feedback. *J. Climate*, **17**, 3661–3665.

Soden, B. J. and I. M. Held, 2005: An assessment of climate feedbacks in coupled ocean-atmosphere models. *J. Climate*, **19**, 3354–3360.

Stephens, G. L., 2005: Cloud feedbacks in the climate system: A critical review. *J. Climate*, **18**, 237–273.

Taylor, K. E., C. D. Hewitt, P. Braconnot, A. J. Broccoli, C. Doutriaux, and J. F. B. Mitchell, 2000: Analysis of forcing, response and feedbacks in a

paleoclimate modeling experiment. *Paleoclimate Modelling Intercomparison Project(PMIP): Proceedings of the Third PMIP Workshop*, P. Braconnot, ed., *WCRP Report WCRP-111*, WMO/TD No. 1007, 43–49.

The GFDL Global Atmospheric Model Development Team, 2004: The new GFDL global atmosphere and land model AM2-LM2: Evaluation with prescribed sst simulations. *J. Climate*, **17**, 4641–4673.

Webb, M. J., C. A. Senior, D. M. H. Sexton, W. J. Ingram, K. D. Williams, M. A. Ringer, B. J. McAvaney, R. Colman, B. J. Soden, R. Gudgel, T. Knutson, S. Emori, T. Ogura, Y. Tsushima, N. G. Andronova, B. Li, I. Musat, S. Bony, K. E. Taylor, 2006: On the contribution of local feedback mechanisms to the range of climate sensitivity in two GCM ensembles. *Clim. Dyn.*, **27**, 17–38.

Wetherald, R. T. and S. Manabe, 1988: Cloud feedback processes in a general circulation model. *J. Atmos. Sci.*, **45**, 1397–1415.

Winton, M., 2005: Simple optical models for diagnosis surface – atmosphere shortwave interactions. *J. Climate*, **18**, 3796–3805.

— 2006: Surface albedo feedback estimates for the AR4 climate models. *J. Climate*, **19**, 359–365.

Yokohata, T., S. Emori, T. Nozawa, Y. Tsushima, T. Ogura, and M. Kimoto, 2005: A simple scheme for climate feedback analysis. *Geophys. Res. Lett.*, **32**, L19703, doi:10.1029/2005GL023673.

Zhang, M. H., R. D. Cess, J. J. Hack, and J. T. Kiehl, 1994: Diagnostic study of climate feedback processes in atmospheric GCMs. *J. Geophys. Res.*, **99**, 5525–5537.

List of Tables

1 Comparison of APRP and PRP calculations of global mean radiative response in a 2xCO_2 experiment. The correlation characterizes the similarity between the spatial patterns of the radiative responses. All other numbers are reported in units of Wm^{-2}. . . . 36

Table 1: Comparison of APRP and PRP calculations of global mean radiative response in a $2xCO_2$ experiment. The correlation characterizes the similarity between the spatial patterns of the radiative responses. All other numbers are reported in units of Wm^{-2}.

	surface albedo	"cloud"	"non-cloud"
radiative response:			
PRP	0.79	-0.63	1.15
APRP	0.72	-0.67	1.24
difference APRP-PRP	-0.07	-0.04	0.09
correlation	0.997	0.997	0.794

List of Figures

1 Schematic representation of a simple shortwave radiation model showing fluxes passing through the atmosphere and being partially reflected on each pass, where S is the insolation, α surface albedo, γ atmospheric scattering coefficient, and $(1-\mu)$ atmospheric absorptance. Wavelengths that are readily absorbed by the atmosphere are assumed to be completely removed on the first pass, and the atmosphere is transparent to other wavelengths. . . 39

2 Surface albedo radiative response (Wm^{-2}) in a CO_2 doubling experiment: a) the APRP estimate and b) the difference between the APRP estimate and the PRP diagnosis of this quantity as in Soden et al. (2004). Note the logarithmic scaling for contour intervals. . 40

3 Shortwave cloud radiative response (Wm^{-2}) in a CO_2 doubling experiment: a) the APRP estimate of the shortwave component of cloud radiative response, b) the difference between the APRP estimate and the PRP diagnosis of this quantity as in Soden et al. (2004), and c) the difference between the change in shortwave cloud forcing and the PRP diagnosis of shortwave cloud radiative response. Note the logarithmic scaling for contour intervals. . . . 41

4 Surface albedo forcing (Wm^{-2}) due to the prescription of ice sheets in last glacial maximum experiments performed with the GFDL and UKMO climate models. The PRP diagnosis (left panels) and APRP estimates (right panels) are provided for the GFDL model (a and b), for the UKMO model (c and d), and for the difference between the two models (e and f). In uncolored regions, there are no ice sheets. 42

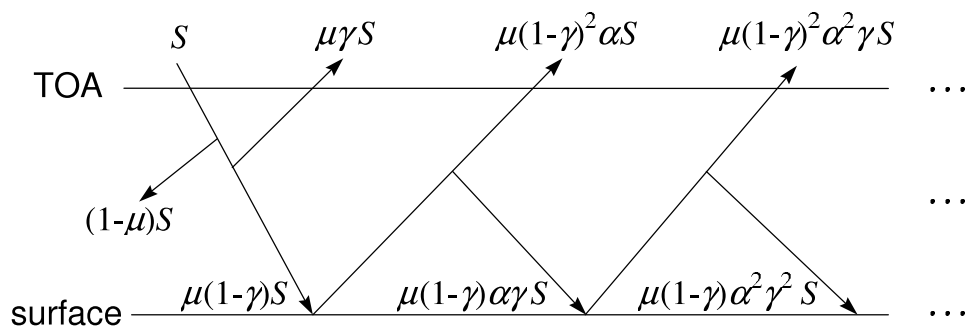

Figure 1: Schematic representation of a simple shortwave radiation model showing fluxes passing through the atmosphere and being partially reflected on each pass, where S is the insolation, α surface albedo, γ atmospheric scattering coefficient, and $(1-\mu)$ atmospheric absorptance. Wavelengths that are readily absorbed by the atmosphere are assumed to be completely removed on the first pass, and the atmosphere is transparent to other wavelengths.

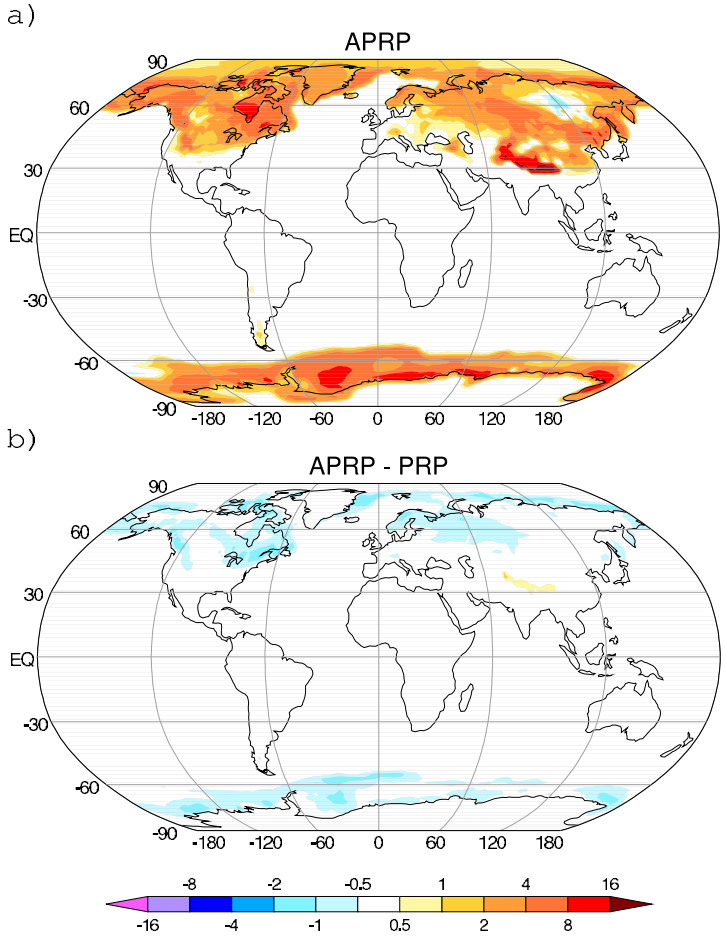

Figure 2: Surface albedo radiative response (Wm^{-2}) in a CO_2 doubling experiment: a) the APRP estimate and b) the difference between the APRP estimate and the PRP diagnosis of this quantity as in Soden et al. (2004). Note the logarithmic scaling for contour intervals.

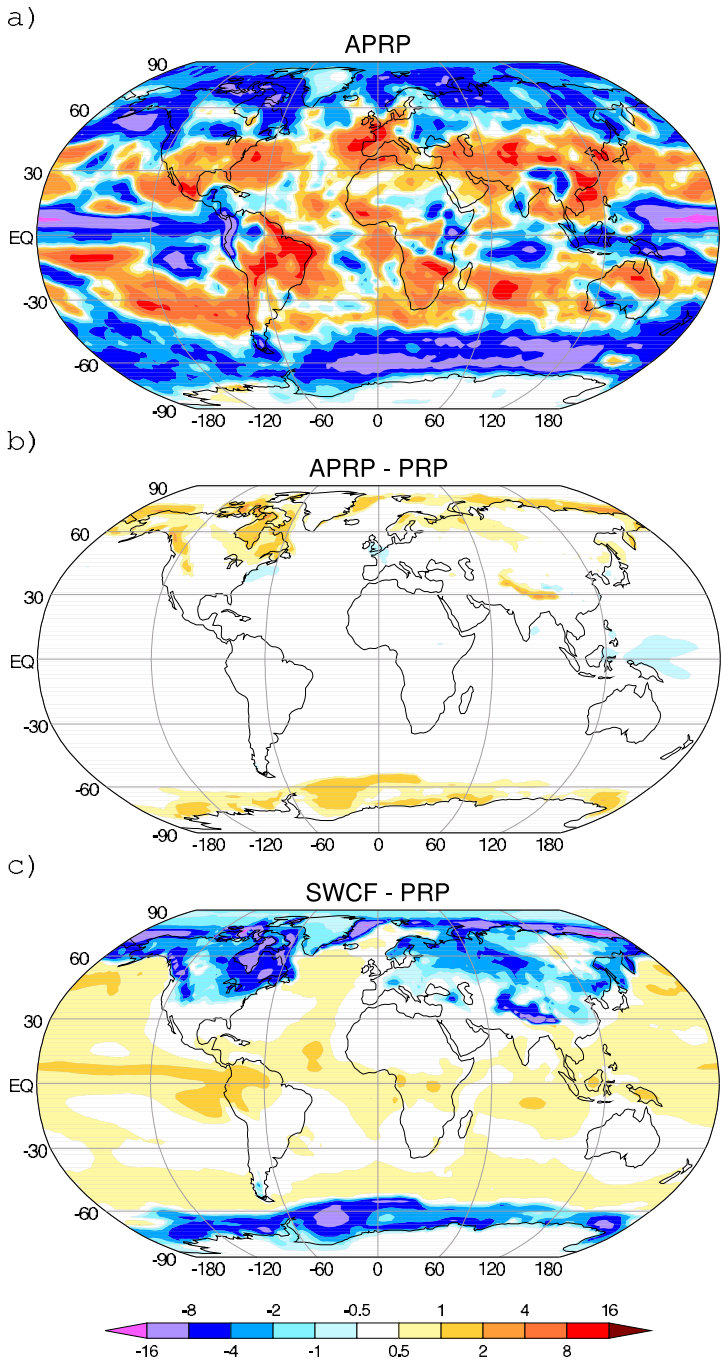

Figure 3: Shortwave cloud radiative response (Wm^{-2}) in a CO_2 doubling experiment: a) the APRP estimate of the shortwave component of cloud radiative response, b) the difference between the APRP estimate and the PRP diagnosis of this quantity as in Soden et al. (2004), and c) the difference between the change in shortwave cloud forcing and the PRP diagnosis of shortwave cloud radiative response. Note the logarithmic scaling for contour intervals.

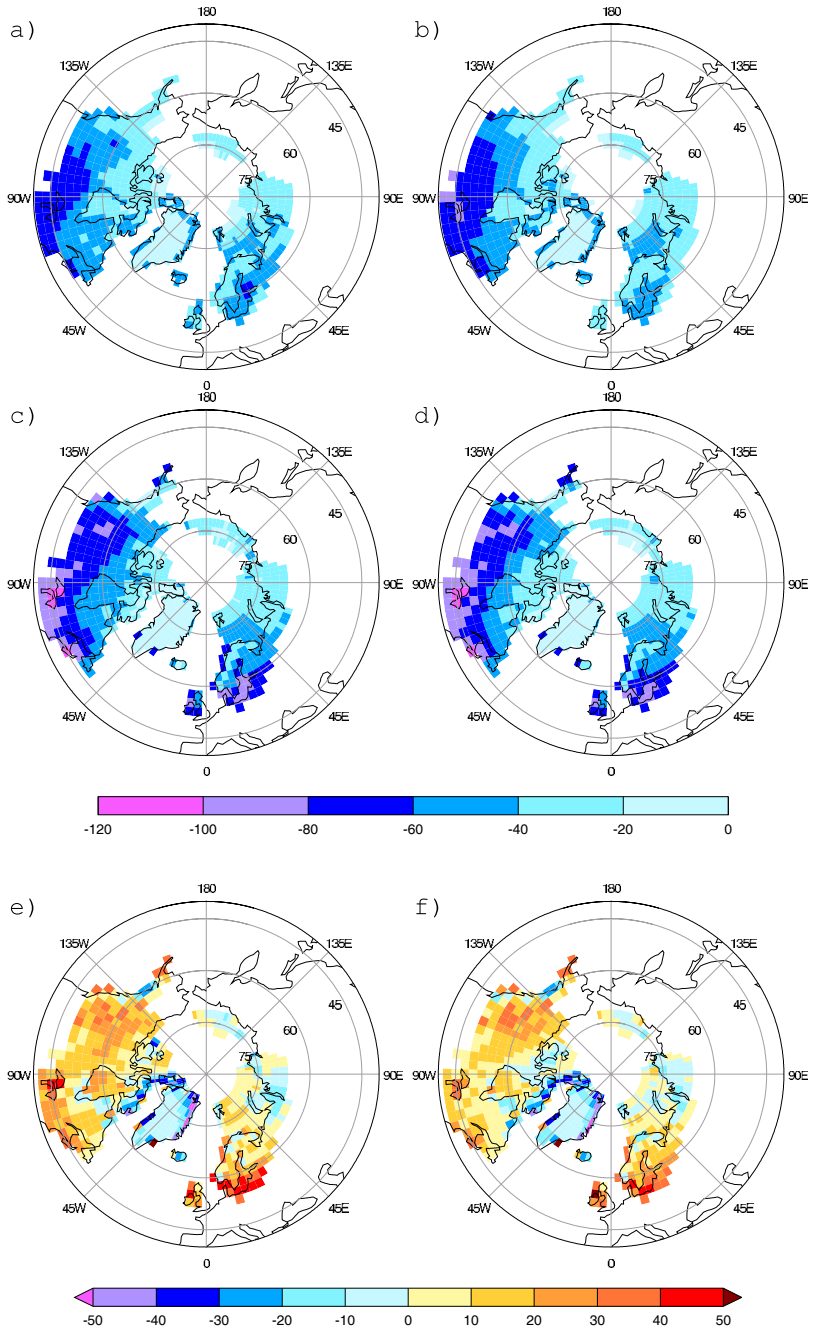

Figure 4: Surface albedo forcing (Wm^{-2}) due to the prescription of ice sheets in last glacial maximum experiments performed with the GFDL and UKMO climate models. The PRP diagnosis (left panels) and APRP estimates (right panels) are provided for the GFDL model (a and b), for the UKMO model (c and d), and for the difference between the two models (e and f). In uncolored regions, there are no ice sheets.